

# A START-TO-END OPTIMISATION STRATEGY FOR THE CompactLight ACCELERATOR BEAMLINE

Y. Zhao\*, A. Latina, CERN, Geneva, Switzerland

A. Aksoy<sup>1</sup>, Ankara University, Ankara, Turkey

H. M. Castaneda Cortes, D. Dunning, N. Thompson

ASTeC and Cockcroft Institute, STFC Daresbury Laboratory, Warrington, United Kingdom

<sup>1</sup>also at CERN, Geneva, Switzerland

## Abstract

The CompactLight collaboration designed a compact and cost-effective hard X-ray FEL facility, complemented by a soft X-ray option, based on X-band acceleration, capable of operating at 1 kHz pulse repetition rate. In this paper, we present a new simple start-to-end optimisation strategy that is developed for the CompactLight accelerator beamline, focusing on the hard X-ray mode. The optimisation is divided into two steps. The first step improves the electron beam quality that finally leads to a better FEL performance by optimising the major parameters of the beamline. The second step provides matched twiss parameters for the FEL undulator by tuning the matching quadrupoles at the end of the accelerator beamline. A single objective optimisation method, with different objective functions, is used to optimise the performance. The sensitivity of the results to jitters is also minimised by including their effects in the final objective function.

## INTRODUCTION

As the fourth and latest generation of synchrotron light source, free-electron-laser (FEL), can produce extremely high brightness radiation, based on linear electron accelerators and undulators. The CompactLight collaboration designed an X-ray FEL facility that is innovative, compact and cost effective, and recently published the Conceptual Design Report (CDR) [1]. In order to significantly reduce the cost and increase the efficiency of the facility, the design aims to bring together recent advances in many of the important technical systems that make up an X-ray FEL.

To meet the requirements from the user community that spreads across a multitude of scientific and engineering disciplines, the facility is supposed to be operated with a large flexibility, with different combinations of soft X-ray (SXR) and hard X-ray (HXR) operating modes, at high and low repetition rates. Two separate FEL beamlines are developed for this purpose:

1. A SXR FEL light source with wavelengths ranging from 5.0 nm to 0.6 nm (0.25 keV to 2 keV) with up to 1 kHz repetition rate.
2. A HXR FEL light source with wavelengths ranging from 0.6 nm to 0.08 nm (2 keV to 16 keV) with maximum 100 Hz repetition rate.

The configuration and operation of the CompactLight FEL are proposed in three stages, including a baseline option and two upgrade options. The baseline configuration satisfies the majority of the user requirements, being able to generate two synchronised photon pulses in Self-Amplified Spontaneous Emission (SASE) mode [2], with either 250 Hz SXR or 100 Hz HXR. Upgrade-1 increases the SXR repetition rate to 1 kHz by using additional klystron power supplies for the accelerating structures while the average RF power is kept constant. Upgrade-2 allows the simultaneous generation of SXR and HXR FEL pulses at 100 Hz.

The required main parameters of the CompactLight FEL are summarised in Table 1. To achieve a good FEL performance and simplify the FEL design, some extra requirements are also considered in the optimisation, such as small transverse shears or offsets (in  $x, y, x', y'$ ) so that the beam centroid is steered on longitudinal axis.

Table 1: Main Parameters of the CompactLight FEL

Parameter	Unit	SXR	HXR
<b>Electrons</b>			
Beam energy	GeV	0.97–1.95	2.75–5.5
Peak current (minimum)	kA	0.35–0.925	1.5–5
RMS sliced energy spread	%	0.02	0.01
RMS sliced emittance	mm-mrad	0.2	
Bunch charge	pC	75	
<b>Photons</b>			
Photon energy	keV	0.25–2	2–16
Wavelength	nm	5–0.6	0.6–0.08
Repetition rate	Hz	250–1000	100

This report presents an optimisation of the accelerator beamline for the HXR mode at the highest beam energy of 5.5 GeV. The beamline to be optimised is displayed in Fig. 1.

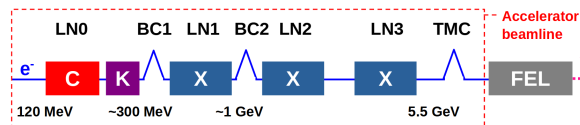


Figure 1: Schematic layout of the beamline to be optimised.

LN0 is Linac-0, consisting of 6 C-band structures, located downstream of a laser heater (LH) and upstream of a K-band lineariser. BC1 and BC2 are magnetic bunch compressors. LN1–3 are Linac-1 to Linac-3, all composed of X-band structures. The designed input beam energy for the optimised

\* yongke.zhao@cern.ch

beamline is ~120 MeV. TMC is a timing chicane followed by the FEL undulators.

Octave [3], RF-Track [4] and PLACET [5] are used for the start-to-end simulation and optimisation. The same configuration and simulation code are used as in the CDR, which has already been preliminarily optimised in ELEGANT [6]. The simulation also takes into consideration the full 6D particle tracking, the space charge effects, coherent synchrotron radiation (CSR) in the bunch compressors, the wakefield effects in the RF linacs and the chromatic effects. We used the “Nelder-Mead simplex method” [7] as the optimisation algorithm, which is a single objective optimisation method in a multi-dimensional space and is named as the “Fminsearch” function in Octave. Therefore, to fulfill all the requirements, different objective functions are defined and combined into one, which is minimised by the optimisation.

## OPTIMISATION STRATEGY

The final objective function used in the optimisation is defined as the quadratic mean ( $M_2$ ) of different “separate” objective functions:

$$F = \sqrt{\sum_{i=1}^n \frac{f_i^2}{n}}, \quad (1)$$

where,  $n$  is the number of objectives required in the optimisation, and  $f_i$  ( $i = 1, 2, \dots, n$ ) represents the “separate” objective functions defined for different FEL requirements. The objective functions that are minimised in the optimisation are defined as follows:

1. Energy:  $f = 30 \cdot |\Delta E|/\text{GeV}$  (if  $\Delta E \leq 0$ ) or  $20 \cdot \Delta E/\text{GeV}$  (if  $\Delta E > 0$ ), where  $\Delta E = \langle E \rangle - 5.5 \text{ GeV}$  is the difference between the mean energy,  $\langle E \rangle$ , of simulated electrons and the required energy 5.5 GeV.
2. Peak current:  $f = 4 \cdot |\Delta I_{\text{peak}}|/\text{kA}$  (if  $|\Delta I_{\text{peak}}| \leq 0.5 \text{ kA}$ ) or  $6 \cdot |\Delta I_{\text{peak}}|/\text{kA}$  (if  $|\Delta I_{\text{peak}}| > 0.5 \text{ kA}$ ), where  $\Delta I_{\text{peak}} = I_{\text{peak}} - 5 \text{ kA}$  is the difference between the peak current of simulated electrons and the required value 5 kA. The peak current is defined as the mean value of the current at the plateau of the sliced distribution.
3. Flat-top:  $f = 12 \cdot \sigma_I^{\text{sliced}} / \langle I^{\text{sliced}} \rangle$ , where  $I^{\text{sliced}}$  is the sliced current at full bunch length. The flat-top or linearised current profile is required such that a maximum number of electrons contribute to the FEL lasing and achieves the maximum FEL brightness. Usually the “Kurtosis” function can be used as the objective function (for example, kurtosis = 1.8 corresponds to a uniform distribution in Octave), but it is found not always to be the case in our study, especially when the bunch is only partially linearised. Therefore a more robust objective function based on the sliced current or bunch charge is used.
4. Energy spread:  $f = \max\{0, 1.2 \times 10^4 \cdot \Delta \frac{\sigma_E}{E}\}$ , where  $\Delta \frac{\sigma_E}{E} = \frac{\sigma_E}{E} - 0.01\%$  is the difference between the sliced

energy spread of simulated electrons and the required value 0.01%.

5. Emittance:  $f = \max\{0, 25 \cdot \Delta \epsilon_{x,y} / (\text{mm} \cdot \text{mrad})\}$ , where  $\Delta \epsilon_{x,y} = \epsilon_{x,y} - 0.15 \text{ mm} \cdot \text{mrad}$  is the difference between the transverse normalised RMS emittance of simulated electrons and the required value 0.15 mm-mrad, which is taken to be an approximation of the input emittance, such that the emittance growth is minimised.
6. Small transverse shear or offset:  $f = 0.4 \cdot \langle |\delta_{x,y}^{\text{sliced}}| \rangle / \mu\text{m}$  or  $0.4 \cdot \langle |\delta_{x',y'}^{\text{sliced}}| \rangle / \mu\text{rad}$ , where  $\delta_{x,y,x',y'}^{\text{sliced}}$  is the sliced transverse beam centroid offset.

The objective functions are defined such that the optimised function values are not much higher than 1 if all requirements are fulfilled, and smaller function values always mean better optimisation results. The number of slices is 100, given that 100,000 electrons are simulated. In addition to the FEL requirements mentioned above, the twiss parameters of the bunch at the end of the beamline need to be matched to the FEL section precisely. Such a requirement is taken into account by combining an additional objective function in a similar way as other requirements, which is defined properly to minimise the difference in twiss parameters.

In case of jitter sensitivity optimisation, jitters are taken into account by extending the final objective function to:

$$F = \langle [2 \cdot F_0, \langle [F_1^{\pm\sigma_1}, F_2^{\pm\sigma_2}, \dots, F_m^{\pm\sigma_m}] \rangle] \rangle, \quad (2)$$

where  $F_0$  is the objective function for a nominal run, and  $F_1, F_2, \dots, F_m$  are for jittered runs. To simplify the optimisation, 2 jittered runs are considered for each source of jitter with  $\pm 1\sigma$  variations, where  $\sigma$  is the RMS jitter error. The jitters considered in this report include: charge variation with  $\sigma = 2\%$ , timing error with  $\sigma = 25 \text{ fs}$ , RF gradient error with  $\sigma = 4\%$ , RF phase error with  $\sigma = 0.05^\circ$ . The jittered function is defined such that the optimisation is dominated by the nominal run but also significantly affected by jitters.

The optimisation is mainly divided into two steps, for either a nominal optimisation or jitter sensitivity optimisation. The first step focuses on the beam quality or FEL performance optimisation by removing the final matching section from the beamline which is located downstream of the TMC. The twiss matching is therefore not considered in the first step. The second step focuses on the twiss matching to the FEL section by optimising only the quadrupoles in the final matching section. This is due to the fact that the twiss parameter matching is required to be precise and therefore dominates the optimisation. The free parameters used in the optimisation include the dipole bending angles, quadrupole strengths and distances between quadrupoles of the matching sections.

## OPTIMISATION RESULTS

The optimisation of the beamline improves the electron beam quality and the FEL performance, especially in transverse phase spaces. The normalised beam emittance growth

is reduced from 0.06 mm-mrad (43%) and 0.01 mm-mrad (7%) to 0.02 mm-mrad (14%) and 0, in horizontal and vertical planes respectively. The beam size and beam centroid offsets along the beamline axis are also reduced significantly, as presented in Fig. 2. The jitter sensitivity is also reduced after the optimisation, especially in transverse phase spaces. With 1000 random jittered runs, the RMS fluctuation of the horizontal beam emittance and beam center offset are reduced from 22.5  $\mu\text{m}\cdot\text{mrad}$  and 2.74  $\mu\text{m}$  to 16.8  $\mu\text{m}\cdot\text{mrad}$  and 1.56  $\mu\text{m}$ , respectively.

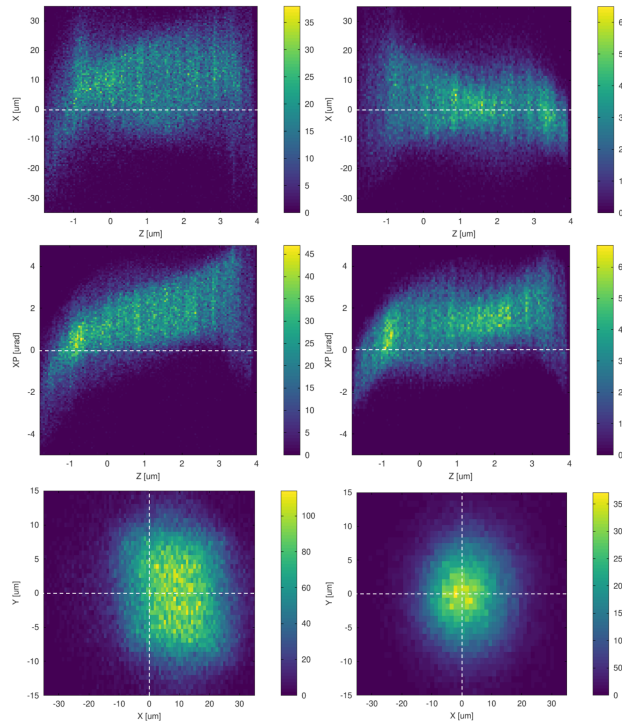


Figure 2: Comparison of electron bunches in transverse phase spaces. Left: before optimisation. Right: after optimisation.

Nominal distributions, before and after optimisation, are imported into the FEL code Genesis 1.3 (v4) [8]. Centroids in  $x$  and  $x'$  are steered onto the undulator axis. For each distribution, 50 independent FEL simulations are performed with different shot noise seeds. After optimisation, the averaged FEL pulse energy at saturation, which is achieved approximately at a distance through the undulator of 27 m, is increased by about 10%, as shown in Fig. 3. The fainter blue and red lines show the individual simulations for Bunch 1 (before optimisation) and Bunch 2 (after optimisation), while the darker lines show the averaged values. Figure 4 shows the characteristic increase in fluctuations as the FEL power develops, then reduction towards saturation [9]. It is seen that the stability of the SASE output is improved after optimisation, with the RMS fluctuation reduced by about 20% at saturation. The reason for this is thought to be that the shot-to-shot stability for SASE is inversely proportional to the square root of number of SASE spikes, and after optimisation the FEL pulse length is longer so that there are more SASE spikes.

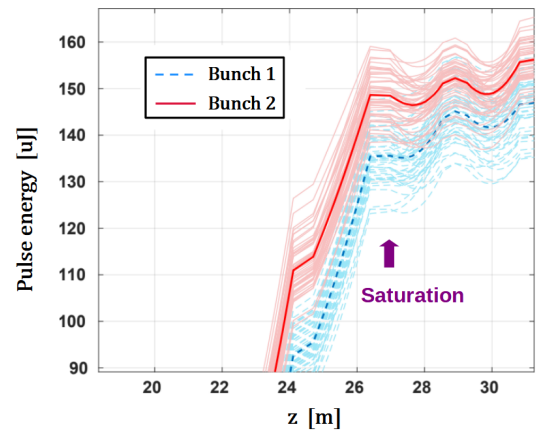


Figure 3: Comparison of FEL pulse energy as a function of the distance through the undulator. Bunch 1: before optimisation. Bunch 2: after optimisation. The shot noise realisations are shown in light colors, while the average values are shown in dark colors.

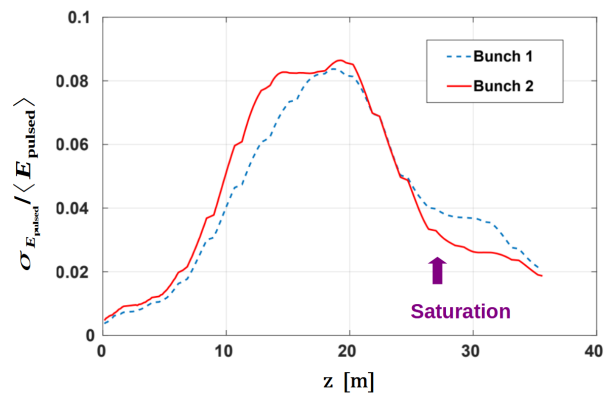


Figure 4: Comparison of FEL pulse energy stability as a function of the distance through the undulator. Bunch 1: before optimisation. Bunch 2: after optimisation.

## SUMMARY

A start-to-end optimisation strategy is developed for the CompactLight accelerator beamline, which is divided into two steps, with the first step focused on the electron beam quality improvement, while the second step focused on the matching to the FEL section. Different objective functions are defined properly for different FEL requirements, and are finally combined into a single function which is then minimised in the optimisation. The sensitivity of the results to jitters is also minimised with an extension of the final objective function. Optimisation results are presented for the hard X-ray mode and show significant improvements in beam quality, jitter sensitivity and FEL performance.

## ACKNOWLEDGEMENT

CompactLight is funded by the European Union's Horizon2020 research and innovation programme under Grant Agreement No. 777431.

## REFERENCES

- [1] G. D'Auria *et al.*, “Conceptual Design Report of the Compact-Light X-ray FEL”, *Zenodo*, 2021. doi:10.5281/zenodo.6375645
- [2] R. Bonifacio *et al.*, “Collective instabilities and high-gain regime in a free electron laser”, *Opt. Commun.*, vol. 50, no. 6, pp. 373–378, 1984. doi:10.1016/0030-4018(84)90105-6
- [3] J. W. Eaton *et al.*, “GNU Octave version 4.2.0 manual: a high-level interactive language for numerical computations”, 2016. <http://www.gnu.org/software/octave/doc/interpreter>
- [4] A. Latina, “RF-Track Reference Manual (2.0.4)”, *Zenodo*, 2020. doi:10.5281/zenodo.3887085
- [5] A. Latina *et al.*, “Evolution of the Tracking Code PLACET”, in *Proc. 4th International Particle Accelerator Conf. (IPAC'13)*, Shanghai, China, May 2013, pp. 1014-1016. <https://jacow.org/IPAC2013/papers/mopwo053.pdf>
- [6] M. Borland, “ELEGANT: A flexible SDDS-compliant code for accelerator simulation”, United States, 2000. doi:10.2172/761286
- [7] J. A. Nelder and R. Mead, “A Simplex Method for Function Minimization”, *Comput. J.*, vol. 7, no. 4, pp. 308–313, 1965. doi:10.1093/comjnl/7.4.308
- [8] S. Reiche, “GENESIS 1.3: A fully 3-D time dependent FEL simulation code”, *Nucl. Instrum. Methods Phys. Res., Sect. A*, vol. 429, no. 1–3, pp. 243–248, 1999. doi:10.1016/S0168-9002(99)00114-X
- [9] G. Brenner *et al.*, “Study of temporal, spectral, arrival time and energy fluctuations of SASE FEL pulses”, *Opt. Express*, vol. 29, no. 7, pp. 10491–10508, 2021. doi:10.1364/OE.419977